Inorganic Chemistry

Article

pubs.acs.org/IC

Coding the Assembly of Polyoxotungstates with a Programmable Reaction System

Andreu Ruiz de la Oliva, Victor Sans, Haralampos N. Miras, De-Liang Long, and Leroy Cronin*

WestCHEM, School of Chemistry, The University of Glasgow, Glasgow G12 8QQ, Scotland, U.K.

Supporting Information

ABSTRACT: Chemical transformations are normally conducted in batch or flow mode, thereby allowing the chemistry to be temporally or spatially controlled, but these approaches are not normally combined dynamically. However, the investigation of the underlying chemistry masked by the self-assembly processes that often occur in one-pot reactions and exploitation of the potential of complex chemical systems requires control in both time and space. Additionally, maintaining the intermediate constituents of a self-assembled system "off equilibrium" and utilizing them dynamically at specific time intervals provide access to building blocks that cannot coexist under one-pot conditions and ultimately to the formation of new clusters. Herein, we implement the concept of a programmable networked reaction system, allowing us to connect discrete "one-pot" reactions that produce the building block$\{W_{11}O_{38}\} \equiv \{W_{11}\}$ under different conditions and control, in real time, the assembly of a series of polyoxometalate clusters $\{W_{12}O_{42}\} \equiv \{W_{12}\}$, $\{W_{22}O_{74}\} \equiv \{W_{22}\}$ **1a**, $\{W_{34}O_{116}\} \equiv \{W_{34}\}$ **2a**, and $\{W_{36}O_{120}\} \equiv \{W_{36}\}$ **3a**, using pH and ultraviolet−visible monitoring. The programmable networked reaction system reveals that is possible to assemble a range of different clusters using $\{W_{11}\}$-based building blocks, demonstrating the relationship between the clusters within the family of iso-polyoxotungstates, with the final structural motif being entirely dependent on the building block libraries generated in each separate reaction space within the network. In total, this approach led to the isolation of five distinct inorganic clusters using a "fixed" set of reagents and using a fully automated sequence code, rather than five entirely different reaction protocols. As such, this approach allows us to discover, record, and implement complex one-pot reaction syntheses in a more general way, increasing the yield and reproducibility and potentially giving access to nonspecialists.

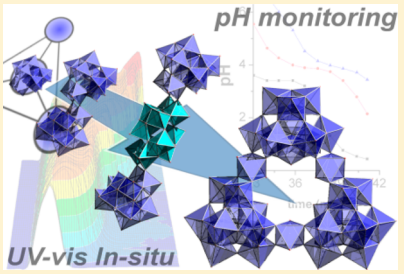

INTRODUCTION

The chemistry of molecular metal oxide polyoxometalate (POM) clusters is a rapidly expanding field because of the vast number of structures, the diversity of their properties,[1−5] and a wide range of potential applications.[6,7] However, the use of one-pot reaction methods[8] for the synthesis of POM clusters[8−11] presents an important problem because it is very hard to understand the crucial steps taking place in solution giving rise to the building blocks, both transient and isolatable, for the assembly of such clusters. In fact, there is currently no general route for exploring one-pot reactions, especially for molecular metal oxides in which real-time kinetics are hard to obtain by nuclear magnetic resonance (NMR) and mass spectrometry. All of these issues mean that it is virtually impossible to devise testable hypotheses regarding the assembly of giant clusters, especially because many of the assembly processes are controlled by complex nonequilibrium kinetics.[12−14] Indeed, it could be that this problem is even more daunting because the one-pot system effectively masks a vast and interconnected range of intricate discrete reactions that underpin the self-assembly process. Furthermore, these issues are also relevant in the solution assembly of other complex molecules such as coordination frameworks[15] and discrete giant metallo-supramolecular[16] architectures.

In this respect, we have recently described the potential for new discoveries by the programmed manipulation of the assembly of some common building blocks in solution[17−19] in an automated fashion. However, with the previous focus being on discovery, there is now a pressing need to develop, and validate, a well-defined platform that incorporates programming and feedback control. Such a setup would allow us to explore different kinetic regimes, reagent combinations, and the control of variables like pH, ionic strength, and redox potential.[20−22] Further, sequential, batch one-by-one conventional one-pot reactions for systematically exploring the POM systems[23,24] and screening the parameter space are very time-consuming and limited in scope, allowing the reactions to be probed only in a comparatively narrow time domain. Most importantly, it is practically impossible to keep a self-assembled system "off equilibrium" or to trap and utilize transient building blocks in batch synthesis.

However, networking reaction systems[25] applied in this case to the assembly of polyoxometalate clusters allow us to test the hypothesis that it is possible to "program" one-pot reactions[26] in both the time and space domains simultaneously (see Figure 1). In this way, the one-pot reaction compositions (r) can be integrated across several different reaction vessels (R_N), simultaneously allowing the convolution of reaction variables ($r \rightarrow R_N$) as a function of fundamental programmable

Received: January 27, 2017
Published: April 17, 2017

DOI: 10.1021/acs.inorgchem.7b00206
Inorg. Chem. 2017, 56, 5089−5095

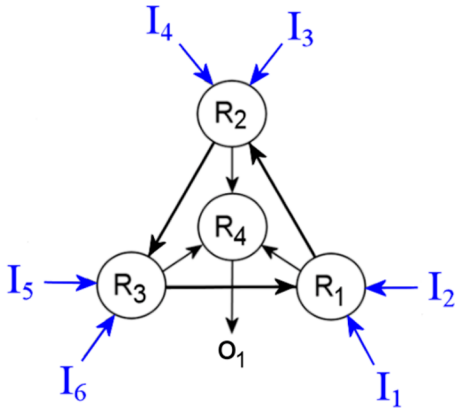

Figure 1. Schematic of our three-connected networked reactor system (R_N, where N = 1, ..., 4) with reagent inlets (I_m, where m = 1, ..., 6) and product outlets (o_j, where j = 1, ...) allowing the generation of time-dependent reaction compositions, r(t) and performance of programmable operations as a function of time, Op(t), such as network pumping (P_{N-N}), inputs (S_{m-N} or S_m), or outputs (O_N or O_{N-j}) (see the Supporting Information for further details).

operations (Op) combining fully automated configurable reactors and externally attached *in situ* analytical techniques [pH, ultraviolet (UV), etc.]. Following these principles, the addition of reactants is denoted by S_m, transferring reaction solutions between reactors by P_{N-N}, and output of reaction solutions by O_N according to the operation sequence (see eq 1).

$$\mathrm{Op}(t)\text{: } \{P_{N-N}, S_{m-N}, O_N\} \quad (1)$$

This means that, by controlling the reaction variables, we should be able to devise new ways to explore and probe one-pot reactions within networked reactor systems, ultimately leading to the discovery and programmable synthesis of molecules using algorithmic control. Indeed, continuous-flow systems have already been used to regulate reaction conditions under pressure,[27−29] and we have also shown how flow-based methods led us to trap a reactive intermediate responsible for the assembly of a gigantic molecular inorganic {Mo_{154}} wheel cluster.[30,31] Because these flow reactor designs were first employed, we have expanded the concept to a new generation of automated digital programmable linear and networked reactor systems; these have led to the discovery and synthesis of gigantic macrocyclic POM architectures such as {Mo_{96}} and {W_{200}}.[26,32]

The purpose of this work was to develop a programmable system that allows the deconvolution of complex systems and compartmentalization of the fundamentally incompatible (with regard to the experimental conditions) individual one-pot reactions for the manipulation of the formed building block libraries, with the ultimate goal being the discovery of new reactivity, mechanism, and compounds. More specifically, we show how a four-connected networked reactor system (a 3,1-NRS) can be used to validate this approach by the synthesis of five different polyoxometalate clusters using a common set of reagents. We also show it is possible to control, in real time, the self-assembly of the common building blocks present in all five clusters using *in situ* analytical techniques that allow us to isolate compounds {W_{11}}, {W_{12}} (paratungstate), {W_{22}}, {W_{34}}, and {W_{36}}.[33,34]

RESULTS AND DISCUSSION

We investigated and integrated the synthesis of a set of iso-polyoxotungstates (iso-POTs)[35] in a single automated system giving $Na_{12}[H_4W_{22}O_{74}]\cdot 50H_2O$ **1**, $Na_{19}[H_9W_{34}O_{116}]\cdot 75H_2O$ **2**,[33] and $(TEAH)_9KNa_2[H_{12}W_{36}O_{120}]\cdot 21H_2O$ **3**.[34,36−38] As such, the NRS allowed us to converge several distinct one-pot reactions using a programmable reaction sequence using one set of common reagents for the *in situ* isolation of {$W_{11}O_{38}$} ≡ {W_{11}}, {$W_{12}O_{42}$} ≡ {W_{12}}, {$W_{22}O_{74}$} ≡ {W_{22}} **1a**, {$W_{34}O_{116}$} ≡ {W_{34}} **2a**, and {$W_{36}O_{120}$} ≡ {W_{36}} **3a**. $[H_4W_{11}O_{38}]^{6-}$ and $[H_5W_{12}O_{42}]^{7-}$ are very well-known iso-POT clusters,[39,40] and compounds **1**−**3** constitute a family of structurally related clusters, namely, the {W_{11}}-based iso-POTs. Compounds **1**−**3** are formed by condensation of building blocks ({W_{11}} and {W_{12}}) (see Figure 2a), synthesized by a programmable pumping sequence, whose reaction conditions were transiently formed, and linked to yield the final cluster

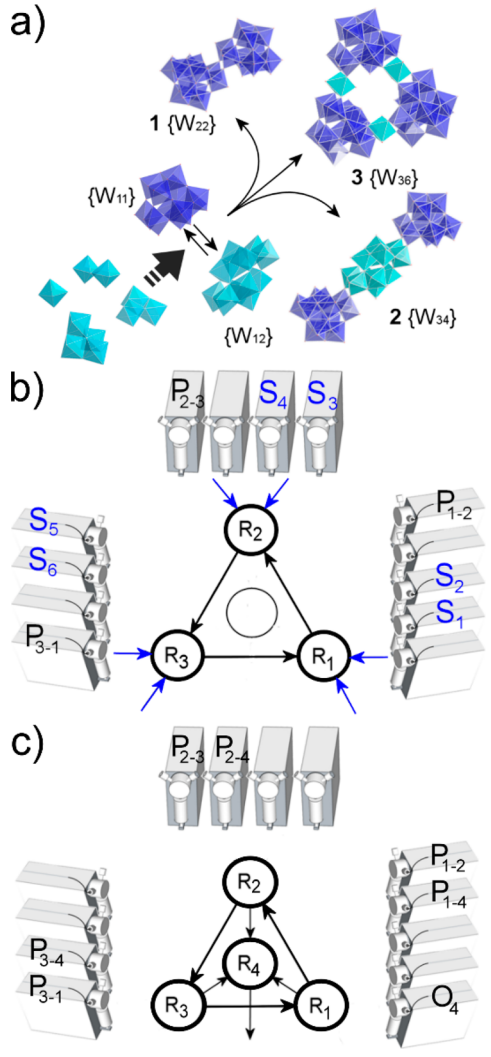

Figure 2. (a) Scheme of the synthetic approach for the synthesis of compounds **1**−**3**. The process starts from a virtual library of the simplest building blocks to form {W_{11}} and {W_{12}} subunits during the acidification process by means of programmable reaction conditions. Two configurations of the reactor system (b and c) correspond to the reaction connectivity of the filling and recycling steps in our approach, respectively. Also, the fundamental programmable operations (P_{N-N}, S_m, and O_N) are specifically assigned to each of the syringe pumps.

DOI: 10.1021/acs.inorgchem.7b00206
Inorg. Chem. 2017, 56, 5089−5095

compounds as outlined above. As described in the literature,[33,40] sodium tungstate dihydrate ($Na_2WO_4{\cdot}2H_2O$) and sodium sulfite (Na_2SO_3) solutions are required to synthesize these clusters using five distinct one-pot reactions. Using the NRS, we aimed to simplify syntheses of these compounds under $(R_1 \rightarrow R_2 \rightarrow R_3)_n$ operation or $R_{1\rightarrow3}$ (Figure 2b).

The experiments were performed in the NRS using three aqueous solutions (I_1 is 6 M HCl, I_4 is 2.4 M Na_2SO_3, and I_5 is 2.8 M $Na_2WO_4{\cdot}2H_2O$) as the main reagents. Moreover, two other stock solutions of amine-based hydrochloride salts [I_3 is 1 M triethanolamine (TEA)·HCl or 1 M dimethylamine (DMA)·HCl] and potassium chloride salt (I_6 is 4.5 M KCl) were also prepared to extend the family to $\{W_{36}O_{120}\}$[25] and $\{W_{11}O_{38}\}$ clusters, using the same networked system (see Table 1), and finally, a H_2O reservoir (I_2) was attached to control the total volume of the final solution.

Table 1. Initial Reaction Conditions Employed in the NRS for the Synthesis of Compounds 1−3

	$\{W_{12}\}$	$\{W_{22}\}$ (**1**)	$\{W_{34}\}$ (**2**)	$\{W_{36}\}$ (**3**)
pH[a]	4.0	3.4	2.4	2.2
$C_{sulfite}$ (M)	0.17	0.17	0.17	–
$C_{tungstate}$ (M)	1.50	1.50	1.50	0.12
C_{KCl} (M)	–	–	–	0.008
C_{TEA} (M)	–	–	–	0.27
t (min)[b]	60	60	60	30
yield (%)[c]	22	23	17	39

[a]pH value for the final solution. [b]Time heating in R_4 at 80 °C. [c]Yield based on tungsten composition.

We wondered whether it is possible to take three separate one-pot reactions, which use same initial reagent composition but produce different cluster building blocks as they are being acidified at different rates. Indeed, we were able to exploit the fact that the $\{W_{12}\}$ cluster has a stability higher than that of the $\{W_{11}\}$ cluster in the presence of sodium cations,[40] and these polyoxometalate clusters are formed at different pH values as the $\{W_{12}\}$ cluster forms at pH >4 and the $\{W_{11}\}$ cluster forms at lower pH values.[39] Thus, by monitoring the pH and controlling the addition of acid, via simultaneous programmable transfer of reagents and acidification, we could observe a gradient of "local" pH changes according to the equation $pH(R_1) < pH(R_2) < pH(R_3)$, which has been previously simulated for three interconnected continuously stirred tanks (see Figure S2). This approach allows us to alternate between near and far-from equilibrium thermodynamic states to determinate populations of the building blocks (BBs) in each reactor, and the hypothesis can be defined by the applied pumping pathways such as $BB(R_1) \rightarrow BB(R_2) \rightarrow BB(R_3)$, according to the pumping regime between the reactors.

The key point in the synthesis of compounds **1**−**3** is controlled by the BB distribution, which is time-dependent, in each $R_{1\rightarrow3}$, which is related to the space-dependent (only in R_1) acidification operation (see Figure 3). Such compounds **1**−**3** were obtained only after a second transfer stage, named the linkage step in R_4, where the pH successively decreases for each compound [**1** at $pH(R_4)$ 3.4, **2** at $pH(R_4)$ 2.4, and **3** at $pH(R_4)$ 2.2]. The isolation of **3** additionally requires the use of organic cations, in this case TEA·HCl.[34] Alternatively, the NRS has the ability to integrate more chemical components because multiple

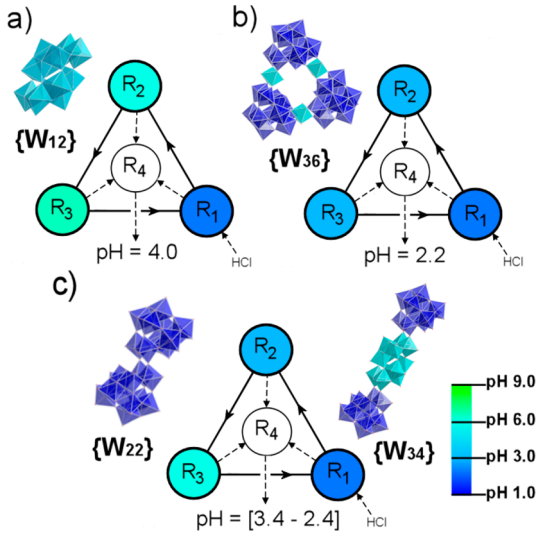

Figure 3. Representation of the NRS of the final cluster, which results from the transfer of cluster building blocks. (a) $\{W_{12}\}$ (paratungstate) appears when $pH(R_4)$ is higher than 3.4, (b) Compound **3** was isolated when $pH(R_4)$ was <2.4. (c) Compounds **1** and **2** are actually isolated within a working pH range of 3.4−2.4.

inputs can be attached to the sequentially connected one-pot approach (Figure 4a).

Then, the hypothesis is specifically formulated by following the BB populations: **1** and **2** by R_1 $\{W_{11}\} \rightarrow \{W_{11}\} + \{W_{12}\} \rightarrow R_2$ $\{W_{12}\}$ and **3** by R_3 $\{W_{11}\} \rightarrow \{W_{11}\} \rightarrow \{W_{11}\}$. Note that $\{W_{11}\}$ is always expected because the acid is being added uniquely into R_1 as giving $\{W_{11}\}$ as the kinetically controlled cluster product. On the other hand, $\{W_{12}\}$ is always produced when the pH is >3.4 because of its high thermodynamic stability under these reaction conditions. To investigate the validity of our hypothesis, we performed a real-time monitoring *in situ* analysis (pH and UV) (Figure 4c) by sequentially ordered operations (see the diagram in Figure 4b). The pH in the three reactors (R_1−R_3) was monitored in parallel by three pH sensors over the 40 min reaction mixture transfer process. Figure 4c shows that pH measurements indicate different local pH values in each reactor, with the same stepped profiles, but shifted in time only because of different acidification rates. The values of $pH(R_2)$ and $pH(R_3)$ can be monitored from the beginning of the process, while $pH(R_1)$ can be measured only ∼30 min after initiation of the experimental procedure, because of the formation of the white precipitate that redissolves after further acidification. In sequence, the addition of acid stops and each of the $R_{1\rightarrow3}$ reactors have different "local" pH values leading to different re-equilibrated BB population distributions. By converging the $R_{1\rightarrow3}$ "one-pot" reactors in the central one (linkage step), we adjusted a suitable "global" pH or $pH(R_4)$ for compounds **1**−**3** when all the components were homogeneously mixed in R_4, heated, and, finally, collected in an open flask.

UV−vis spectrometry was also used to monitor the reaction during the pumping sequence between reactors, showing how the UV bands evolve with the acidification process (Figure 5a). The band at 330 nm, assigned to $\{W_{11}\}$ cluster formation (see Figure S6), was monitored in R_2 and R_3 simultaneously (Figure 5b), and the UV profiles are shifted in a time-dependent fashion. Hence, by dipping UV probes into every single "one-pot" reactor, we observed the formation of $\{W_{11}\}$ on a different

DOI: 10.1021/acs.inorgchem.7b00206
Inorg. Chem. 2017, 56, 5089−5095

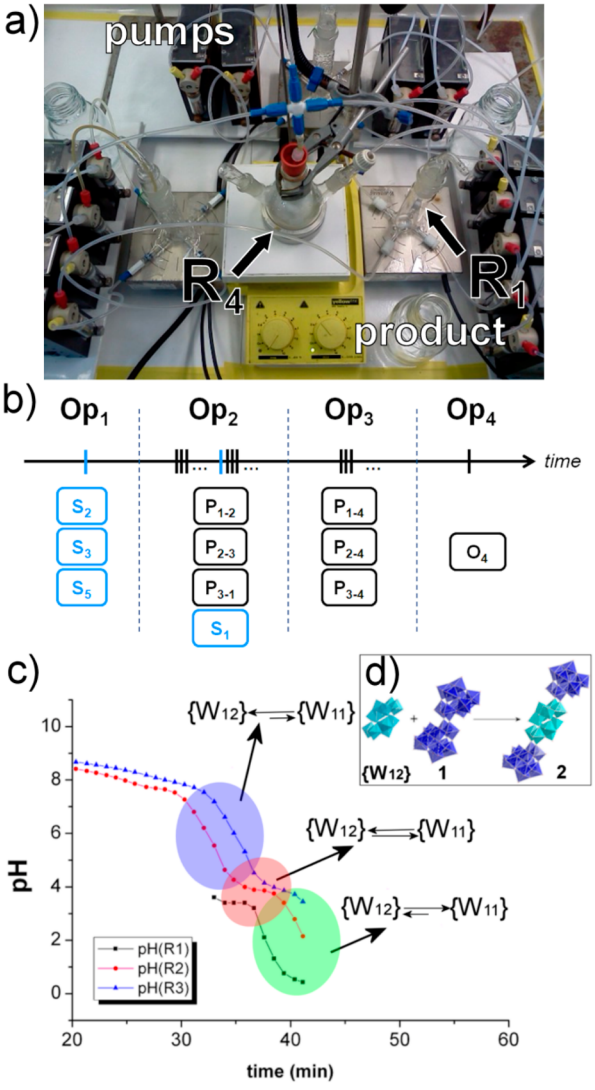

Figure 4. (a) Picture of the NRS in which the local pH is controlled and monitored as a function of time in each reactor for the synthesis of compounds **1**–**5**. (b) Diagram of the NRS method for the synthesis of compound **2**, in terms of the sequence of operation (input, S; networking, P; outputs, O). (c) Monitoring of the pH allows us to observe a stepped profile (red) that corresponds to equal building cluster populations, as well as nonequal states (blue and green) in the different reactors during the process. (d) In the synthesis of compound **2**, the increase in the $\{W_{11}\}$ population allowed the entrapment of a single $\{W_{12}\}$ (paratungstate) cluster between two $\{W_{11}\}$ clusters.

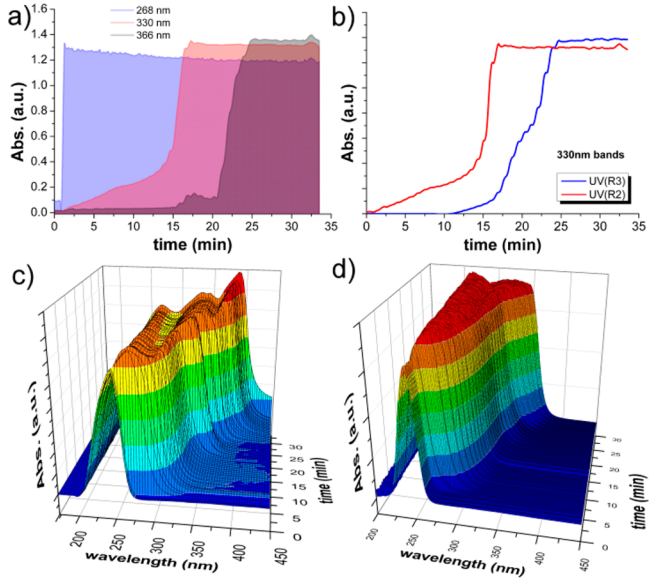

Figure 5. UV monitoring during the synthesis of compound **2**. (a) The profile plot (smoothed) for R_2 compares three different peaks appearing at different time scales. (b) UV profiles (smoothed) of the band at 330 nm in R_2 (red) and R_3 (deep blue). Two three-dimensional plots of UV spectra vs time are shown for (c) R_2 and (d) R_3, allowing us to observe the evolution of the UV spectra in relation to the pumping sequence.

time scale, for instance comparing R_2 to R_3 (Figure 5c,d). The mechanistic studies are an interesting aspect to consider because reactor R_2 may be affected and gradually populated by the $\{W_{11}\}$ clusters, allowing the synthesis of **2** by reaction of $\{W_{12}\}$ and **1** (see Figure 4d). Indeed, the study of the self-assembly processes has allowed us to reconsider the role of the $\{W_{11}\}$ as a key building block. As described previously, subunit $\{W_{11}\}$ is commonly found within these structures despite it is being difficult to isolate. Lehmann and Fuchs described this cluster in 1988, but the procedure is very hard to reproduce.[39] However, using mechanistic observations explained above, we found that the $\{W_{11}\}$ building block can be obtained very efficiently by adding a large excess of KCl during the synthesis of $\{W_{22}\}$ [this is a modification of the previously reported "batch" synthesis (see the Supporting Information)]. This new methodology also gives a rational explanation of the formation of **1** that takes place by the condensation of two $\{W_{11}\}$ clusters. The configurability of the NRS allowed sequential addition of the KCl stock solution at different concentrations directly in the final mixture following the performance of the $R_3 \rightarrow R_4$ sequence.

However, instead of isolating the $[H_4W_{11}O_{38}]^{6-}$ anion in an attempt to reproduce the synthesis of the $\{W_{11}\}$ cluster, we isolated an unexpected K^+-containing $\{W_{22}\}$ cluster (K_8Na_4**1a**·$31H_2O$ **4**). In fact, compound **4** seems to be an intermediate state between $\{W_{11}\}$ and **1**, which can be isolated because of the transient dilution states of the one-pot reactors that stabilize the $\{W_{22}\}$ species in the presence of lower concentrations of K^+ cations [1 M under NRS conditions vs 3.35 M under "one-pot" conditions (see the Supporting Information for synthesis of the $\{W_{11}\}$ building block)]. It is worth noting that at higher concentrations the presence of potassium cations tends to disintegrate the $\{W_{22}\}$ species to its constituents, which is the $\{W_{11}\}$ BB. These observations helped us to validate the idea that the $\{W_{11}\}$ cluster is capable of "trapping" species from solution, such as $\{W_{12}\}$ or $\{W_1\}$, yielding compound **2** or **3**, respectively, and even transition metal cations, such as $\{Co(H_2O)_6\}^{2+}$, as observed in the case of $\{W_{22}Co\}$.[26]

Other aspects of this particular reaction system are efficiency and reliability, which we can change with the counterions; this is very interesting because it is often very difficult, if not impossible, to change the counterions in the normal one-pot synthesis of a polyoxometalate without affecting the synthesis or structure formed. For instance, by using the same programmable reaction protocol that was applied while the TEA was replaced by a stock solution of DMA, we isolated $(DMAH)_9KNa_2$**3a**·$22H_2O$ **5** (anions **3a** are isostructural, although they crystallize in distinct unit cells).[34] These results suggest that the compounds presented in this work are related by a network of underlying reactions between the $\{W_{11}\}$ and

DOI: 10.1021/acs.inorgchem.7b00206
Inorg. Chem. 2017, 56, 5089−5095

{W_{12}} BBs. The formation of these compounds has previously been justified entirely by the existence of a "virtual combinatorial library" of tungstate aggregates based on crystallographic observations. It is has long been suggested that large clusters must be assembled in solution from a series of smaller so-called building blocks accessible from a virtual combinatorial library of common building blocks.[41]

The use of automated control of networked "one-pot" reactor systems allows us to test this idea of far-from equilibrium reaction conditions operating in volume transfer, flow rates, and pumping frequency basis (Figure 6). In this

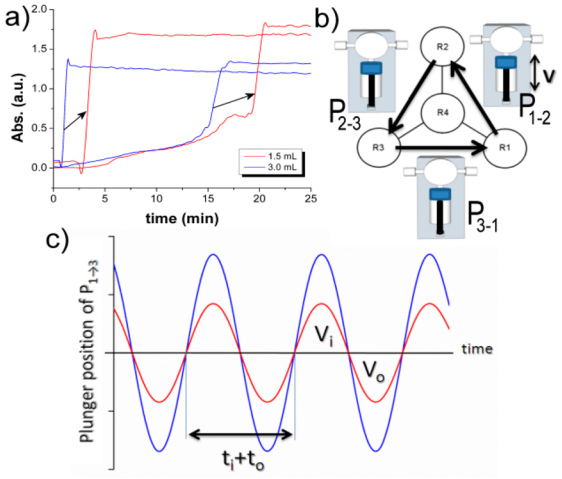

Figure 6. Evaluation of the volume effect during UV monitoring. (a) A decreasing volume leads a shift of the main peaks in the UV spectra. (b) Scheme of the NRS during the pumping pathway, employing operations P_{1-2}, P_{2-3}, and P_{3-1}. (c) Plot of the plunger position vs time, showing how the volume oscillates along input−output alternating sequences and the flow rate becomes the operation rate when using syringe pumps in sequence.

sense, the future potential of the NRS is focused on the exploration of not only multiconnectivity and configurability between the formation of transient $N \geq 5$ "one-pot" reactors but also different pumping regimes and reaction conditions in a programmed and sequential way (giving access to new compounds with the same "space synthesis" but with a different "time synthesis"). This feature makes the NRS unique and potentially very useful in mechanistic studies and self-assembly of labile coordination or organic clusters[42] to achieve only-NRS accessible exotic products (kinetically unstable units co-trapped giving dynamic kinetic stability), such as giant supramolecular architectures.[43−45] Finally, we postulate that it would be interesting to utilize the NRS to explore n times the same one-pot reactions as a function of time (r_t), where aliquots of r_{t+1} could be used to seed r_{t-1}, thereby allowing a future "template" to be reseeded to previous or "past" reaction conditions. This would lead to a real prospect that novel compounds could be generated by a pumping frequency-dependent reseeding approach using future information intrinsic to the system to disturb a past version of the system with a higher concentration of unlinked or exploited building blocks.

CONCLUSIONS

In conclusion, the NRS is used to integrate distinct syntheses of structurally related clusters, by multiple one-pot connected reactions. The common reaction variables were explored because of the NRS, which facilitates the automation of the syntheses of compounds **1**−**5**. The NRS allowed us to modulate chemical compositions and an efficient pH adjustment during the application of a reaction protocol, thus producing different experimental conditions in each reactor within the system. As such, we propose a rational synthetic explanation (Figure 6) for the isolation of such isopolyoxometalates based on {W_{11}} and {W_{12}} building blocks (BBs) formed in separate reactors. The hypothesis has been probed by using pH and UV real-time control to identify and monitor populations of transient species or building clusters, validating in a very basic sense the idea of a POM-based dynamic library.

In future work, we will extend the NRS approach to generate "sequence codes" for the synthesis of new compounds and reactive species from a given NRS connectivity with a predefined reagent set. We will also devise a standard reactor format suitable for cost-effective open-source duplication. This raises the real possibility of vastly expanding the exploration of one-pot synthesis, across a variety of chemistries, for the isolation of industrially useful and functional materials that can be reliably synthesized on a large scale without highly specialized know-how from sequence codes and an open-source reactor format.

EXPERIMENTAL SECTION

Synthesis. All experiments are based on the operation of the networked reactor system, followed by regular analytics to fully characterize compounds **1**−**5**. Crystal data and structure refinements are available for the following compounds. $K_8Na_4[H_4W_{22}O_{74}]\cdot 31H_2O$ (**4**): $H_{66}K_8Na_4O_{105}W_{22}$; M_r = 6195.99 g mol^{-1}; colorless long crystal; monoclinic; space group $C2/c$; a = 40.2229(16) Å; b = 12.7409(5) Å; c = 19.5968(8) Å; β = 112.8562(7)°; V = 9254.3(6) Å^3; Z = 4; ρ = 4.447 g cm^{-3}; λ(Mo Kα) = 0.71073 Å; 50632 reflections measured; 8492 unique reflections (R_{int} = 0.0632) that were used in all calculations; 441 refined parameters; final R_1 = 0.0574 and wR_2 = 0.1736 (all data). $(DMAH)_9KNa_2[H_{12}W_{36}O_{120}]\cdot 22H_2O$ (**5**): $C_{18}H_{128}KN_9Na_2O_{142}W_{36}$; M_r = 9446.97 g mol^{-1}; colorless long crystal; monoclinic; space group $C2/c$; a = 37.3679(17) Å; b = 26.2614(17) Å; c = 35.8129(14) Å; β = 118.486(7)°; V = 30890(3) Å^3; Z = 8; ρ = 4.063 g cm^{-3}; λ(Mo Kα) = 0.71073 Å; 131486 reflections measured; 30320 unique reflections (R_{int} = 0.1252) that were used in all calculations; 1682 refined parameters; final R_1 = 0.0540 and wR_2 = 0.1241 (all data). Data collection and reduction were performed using the CrysAlis software package, and structure solution and refinement were performed using the SHELXS-97 and SHELXL-97[46,47] program package of WINGX.[48] Corrections for incident and diffracted beam absorption effects were applied using empirical absorption correction. CCDC 982262 (**4**) and 982261 (**5**) contain the supplementary crystallographic data for this paper. These data can be obtained from The Cambridge Crystallographic Data Centre via http://www.ccdc.cam.ac.uk/.

UV-Integrated Networked Reactor System. The NRS presented here is assembled from 13 pumps; six of these are used to introduce the initial stock solutions of each reagent, and the other six are used for transferring the reaction mixtures and interconnecting the four stirred reactors. Finally, one pump is used to extract the final reaction mixture for collection. The current setup uses programmable syringe pumps (C3000 model, Tritontinent Ltd.) and a LabVIEW-based PC interface for the real-time monitoring and control of the setup.

***In Situ* Monitoring.** The pH control was performed in the three primary reactors simultaneously using SevenMulti Mettler Toledo double-instant pH-meters. UV monitoring was performed simultaneously in R_2 and R_3 using a second LabVIEW PC interface connected to the Avantes Avaspec-2048 spectrometer equipped with a DH-2000

DOI: 10.1021/acs.inorgchem.7b00206
Inorg. Chem. 2017, 56, 5089−5095

halogen light source (Oceanoptics) that was connected further through a fiber-optic cable to a TP300 fiber probe.

■ ASSOCIATED CONTENT

Supporting Information

The Supporting Information is available free of charge on the ACS Publications website at DOI: 10.1021/acs.inorgchem.7b00206.

Experimental procedures, including full details of the NRS system, including pumps, control, and configuration (PDF)
Crystallographic data (CIF)
CheckCIF/PLATON report (PDF)
Crystallographic data (CIF)

■ AUTHOR INFORMATION

Corresponding Author

*E-mail: Lee.Cronin@glasgow.ac.uk.

ORCID

Victor Sans: 0000-0001-7045-5244
Haralampos N. Miras: 0000-0002-0086-5173
Leroy Cronin: 0000-0001-8035-5757

Funding

This work was supported by the EPSRC (Grants EP/H024107/1, EP/I033459/1, and EP/J015156/1), the University of Glasgow, and the ERC (Project 670467 SMART-POM). L.C. thanks the Royal-Society Wolfson Foundation for a Merit Award.

Notes

The authors declare no competing financial interest.

■ ACKNOWLEDGMENTS

We thank Dr. Craig J. Richmond and Niall Mclean for useful discussions.

■ REFERENCES

(1) Rezaeifard, A.; Haddad, R.; Jafarpour, M.; Hakimi, M. Catalytic Epoxidation Activity of Keplerate Polyoxomolybdate Nanoball toward Aqueous Suspension of Olefins under Mild Aerobic Conditions. *J. Am. Chem. Soc.* **2013**, *135*, 10036−10039.

(2) Kortz, U.; Müller, A.; van Slageren, J.; Schnack, J.; Dalal, N. S.; Dressel, M. Polyoxometalates: Fascinating structures, unique magnetic properties. *Coord. Chem. Rev.* **2009**, *253*, 2315−2327.

(3) Biboum, R. N.; Njiki, C. P. N.; Zhang, G.; Kortz, U.; Mialane, P.; Dolbecq, A.; Mbomekalle, I. M.; Nadjo, L.; Keita, B. High nuclearity Ni/Co polyoxometalates and colloidal TiO_2 assemblies as efficient multielectron photocatalysts under visible or sunlight irradiation. *J. Mater. Chem.* **2011**, *21*, 645−650.

(4) Fang, X.; Luban, M. $\{Mn_{14}W_{48}\}$ aggregate: the perspective of isopolyanions as ligands. *Chem. Commun.* **2011**, *47*, 3066−3068.

(5) Gaspar, A. R.; Gamelas, J. A. F.; Evtuguin, D. V.; Pascoal Neto, C. Alternatives for lignocellulosic pulp delignification using polyoxometalates and oxygen: a review. *Green Chem.* **2007**, *9*, 717−730.

(6) Miras, H. N.; Yan, J.; Long, D.-L.; Cronin, L. Engineering polyoxometalates with emergent properties. *Chem. Soc. Rev.* **2012**, *41*, 7403−7430.

(7) Botar, B.; Kögerler, P.; Hill, C. L. Tetrairon and hexairon hydroxo/acetato clusters stabilized by multiple polyoxometalate scaffolds. structures, magnetic properties, and chemistry of a dimer and a trimer. *Inorg. Chem.* **2007**, *46*, 5398−5403.

(8) Feng, X.-J.; Han, H.-Y.; Wang, Y.-H.; Li, L.-L.; Li, Y.-G.; Wang, E.-B. Assembly of chainlike polyoxometalate-based lanthanide complexes in one-pot reaction system. *CrystEngComm* **2013**, *15*, 7267−7273.

(9) Kikukawa, Y.; Yamaguchi, K.; Hibino, M.; Mizuno, N. Layered assemblies of a dialuminum-substituted silicotungstate trimer and the reversible interlayer cation-exchange properties. *Inorg. Chem.* **2011**, *50*, 12411−12413.

(10) Proust, A.; Matt, B.; Villanneau, R.; Guillemot, G.; Gouzerh, P.; Izzet, G. Functionalization and post-functionalization: a step towards polyoxometalate-based materials. *Chem. Soc. Rev.* **2012**, *41*, 7605−7622.

(11) Mbomekalle, I. M.; Keita, B.; Nadjo, L.; Berthet, P.; Hardcastle, K. I.; Hill, C. L.; Anderson, T. M. Multi-Iron Tungstodiarsenates. Synthesis, Characterization, and Electrocatalytic Studies of $\alpha\beta\beta\alpha$-$(Fe^{III}OH_2)_2Fe^{III}_2(As_2W_{15}O_{56})_2^{12-}$. *Inorg. Chem.* **2003**, *42*, 1163−1169.

(12) Merca, A.; Garai, S.; Bögge, H.; Haupt, E. T. K.; Ghosh, A.; López, X.; Poblet, J. M.; Averseng, F.; Che, M.; Müller, A. An Unstable Paramagnetic Isopolyoxomolybdate Intermediate Non-Homogeneously Reduced at Different Sites and Trapped in a Host Based on Chemical Adaptability. *Angew. Chem., Int. Ed.* **2013**, *52*, 11765−11769.

(13) Fang, X.; Hansen, L.; Haso, F.; Yin, P.; Pandey, A.; Engelhardt, L.; Slowing, I.; Li, T.; Liu, T.; Luban, M.; Johnston, D. C. $\{Mo_{24}Fe_{12}\}$ macrocycles: anion templation with large polyoxometalate guests. *Angew. Chem., Int. Ed.* **2013**, *52*, 10500−10504.

(14) Fang, X.; Kögerler, P.; Furukawa, Y.; Speldrich, M.; Luban, M. Molecular growth of a core−shell polyoxometalate. *Angew. Chem., Int. Ed.* **2011**, *50*, 5212−5216.

(15) Deng, H.; Doonan, C. J.; Furukawa, H.; Ferreira, R. B.; Towne, J.; Knobler, C. B.; Wang, B.; Yaghi, O. M. Multiple functional groups of varying ratios in metal-organic frameworks. *Science* **2010**, *327*, 846.

(16) Campbell, V. E.; de Hatten, X.; Delsuc, N.; Kauffmann, B.; Huc, I.; Nitschke, J. R. Cascading transformations within a dynamic self-assembled system. *Nat. Chem.* **2010**, *2*, 684−687.

(17) Atcher, J.; Moure, A.; Alfonso, I. The emergence of halophilic evolutionary patterns from a dynamic combinatorial library of macrocyclic pseudopeptides. *Chem. Commun.* **2013**, *49*, 487−489.

(18) Moulin, E.; Cormos, G.; Giuseppone, N. Dynamic combinatorial chemistry as a tool for the design of functional materials and devices. *Chem. Soc. Rev.* **2012**, *41*, 1031−1049.

(19) Hunt, R. A. R.; Otto, S. Dynamic combinatorial libraries: new opportunities in systems chemistry. *Chem. Commun.* **2011**, *47*, 847−858.

(20) Miras, H. N.; Raptis, R. G.; Lalioti, N.; Sigalas, M. P.; Baran, P.; Kabanos, T. A. A Novel Series of Vanadium−Sulfite Polyoxometalates: Synthesis, Structural, and Physical Studies. *Chem. - Eur. J.* **2005**, *11*, 2295−2306.

(21) Streb, C. New trends in polyoxometalate photoredox chemistry: From photosensitisation to water oxidation catalysis. *Dalton Trans.* **2012**, *41*, 1651−1659.

(22) Kögerler, P.; Tsukerblat, B.; Müller, A. Structure-related frustrated magnetism of nanosized polyoxometalates: aesthetics and properties in harmony. *Dalton Trans.* **2010**, *39*, 21−36.

(23) Forster, J.; Rosner, B.; Khusniyarov, M. M.; Streb, C. Tuning the light absorption of a molecular vanadium oxide system for enhanced photooxidation performance. *Chem. Commun.* **2011**, *47*, 3114−3116.

(24) Botar, B.; Ellern, A.; Kögerler, P. Mapping the formation areas of giant molybdenum blue clusters: a spectroscopic study. *Dalton Trans.* **2012**, *41*, 8951−8959.

(25) Yuan, Z.; Zhao, C.; Di, Z.; Wang, W.-X.; Lai, Y.-C. Exact controllability of complex networks. *Nat. Commun.* **2013**, *4*, 2447.

(26) de la Oliva, A. R.; Sans, V.; Miras, H. N.; Yan, J.; Zang, H.; Richmond, C. J.; Long, D.-L.; Cronin, L. Assembly of a gigantic polyoxometalate cluster $\{W_{200}Co_8O_{660}\}$ in a networked reactor system. *Angew. Chem., Int. Ed.* **2012**, *51*, 12759−12762.

(27) Moore, J. S.; Jensen, K. E. Batch" kinetics in flow: online IR analysis and continuous control. *Angew. Chem., Int. Ed.* **2014**, *53*, 470−473.

(28) Wegner, J.; Ceylan, S.; Kirschning, A. Flow chemistry−a key enabling technology for (multistep) organic synthesis. *Adv. Synth. Catal.* **2012**, *354*, 17−57.

DOI: 10.1021/acs.inorgchem.7b00206
Inorg. Chem. 2017, 56, 5089−5095

(29) Yoshida, J.-i.; Takahashi, Y.; Nagaki, A. Flash chemistry: flow chemistry that cannot be done in batch. *Chem. Commun.* **2013**, *49*, 9896−9904.
(30) Miras, H. N.; Cooper, G. J. T.; Long, D.-L.; Bögge, H.; Müller, A.; Streb, C.; Cronin, L. Unveiling the transient template in the self-assembly of a molecular oxide nanowheel. *Science* **2010**, *327*, 72−74.
(31) Miras, H. N.; Richmond, C. J.; Long, D.-L.; Cronin, L. Solution-phase monitoring of the structural evolution of a molybdenum blue nanoring. *J. Am. Chem. Soc.* **2012**, *134*, 3816−3824.
(32) Richmond, C. J.; Miras, H. N.; de la Oliva, A. R.; Zang, H.; Sans, V.; Paramonov, L.; Makatsoris, H.; Inglis, R.; Brechin, E. K.; Long, D.-L.; Cronin, L. A flow-system array for the discovery and scale up of inorganic clusters. *Nat. Chem.* **2012**, *4*, 1037−1043.
(33) Miras, H. N.; Yan, J.; Long, D.-L.; Cronin, L. Structural Evolution of "S"−Shaped $[H_4W_{22}O_{74}]^{12-}$ and "§ "−Shaped $[H_{10}W_{34}O_{116}]^{18-}$ Isopolyoxotungstate Clusters. *Angew. Chem., Int. Ed.* **2008**, *47*, 8420−8423.
(34) Long, D.-L.; Abbas, H.; Kögerler, P.; Cronin, L. A High-Nuclearity "Celtic-Ring" Isopolyoxotungstate, $[H_{12}W_{36}O_{120}]^{12-}$, That Captures Trace Potassium Ions. *J. Am. Chem. Soc.* **2004**, *126*, 13880−13881.
(35) Ban, T.; Ito, T.; Ohya, Y. Phase Transition between Layered Tungstates and Polyoxotungstates in Aqueous Solutions. *Inorg. Chem.* **2013**, *52*, 10520−10524.
(36) Long, D.-L.; Brücher, O.; Streb, C.; Cronin, L. Inorganic crown: the host−guest chemistry of a high nuclearity 'Celtic-ring'isopolyoxotungstate $[H_{12}W_{36}O_{120}]^{12-}$. *Dalton Trans.* **2006**, 2852−2860.
(37) Streb, C.; McGlone, T.; Brücher, O.; Long, D.-L.; Cronin, L. Hybrid host−guest complexes: directing the supramolecular structure through secondary host−guest interactions. *Chem. - Eur. J.* **2008**, *14*, 8861−8868.
(38) McGlone, T.; Streb, C.; Long, D.-L.; Cronin, L. Guest-Directed Supramolecular Architectures of {W-36} Polyoxometalate Crowns. *Chem. - Asian J.* **2009**, *4*, 1612−1618.
(39) Lehmann, T.; Fuchs, J. Struktur und Schwingungsspektrum des Kaliumundecawolframats $kg_6H_4W_{11}O_{38}\cdot 11H_2O$/Structure and Vibrational Spectrum of the Potassium Undecatungstate $K_6H_4WnO_{38}$ −11 H_2O. *Z. Naturforsch., B: J. Chem. Sci.* **1988**, *43*, 89−93.
(40) Chrissafidou, A.; Fuchs, J.; Hartl, H.; Palm, R. Kristallisation und Strukturuntersuchung von Alkali-Parawolframaten/Crystallization and Structure Determination of Alkaline Metal-Paratungstates. *Z. Naturforsch., B: J. Chem. Sci.* **1995**, *50*, 217−222.
(41) Müller, A.; Kögerler, P.; Kuhlmann, C. A variety of combinatorially linkable units as disposition: from a giant icosahedral Keplerate to multi-functional metal−oxide based network structures. *Chem. Commun.* **1999**, 1347−1358.
(42) Yoneya, M.; Yamaguchi, T.; Sato, S.; Fujita, M. Simulation of metal−ligand self-assembly into spherical complex M_6L_8. *J. Am. Chem. Soc.* **2012**, *134*, 14401−14407.
(43) Black, S. P.; Stefankiewicz, A. R.; Smulders, M. M. J.; Sattler, D.; Schalley, C. A.; Nitschke, J. R.; Sanders, J. K. M. Generation of a Dynamic System of Three-Dimensional Tetrahedral Polycatenanes. *Angew. Chem., Int. Ed.* **2013**, *52*, 5749−5752.
(44) Parera, E.; Comelles, F.; Barnadas, R.; Suades, J. Formation of vesicles with an organometallic amphiphile bilayer by supramolecular arrangement of metal carbonyl metallosurfactants. *Chem. Commun.* **2011**, *47*, 4460−4462.
(45) Newton, G. N.; Onuki, T.; Shiga, T.; Noguchi, M.; Matsumoto, T.; Mathieson, J. S.; Nihei, M.; Nakano, M.; Cronin, L.; Oshio, H. Mapping the Sequential Self−Assembly of Heterometallic Clusters: From a Helix to a Grid. *Angew. Chem., Int. Ed.* **2011**, *50*, 4844−4848.
(46) Sheldrick, G. M. Phase annealing in SHELX-90: direct methods for larger structures. *Acta Crystallogr., Sect. A: Found. Crystallogr.* **1990**, *46*, 467−473.
(47) Sheldrick, G. M. Crystal structure refinement with SHELXL. *Acta Crystallogr., Sect. A: Found. Crystallogr.* **2008**, *64*, 112−122.
(48) Farrugia, L. J. WinGX suite for small-molecule single-crystal crystallography. *J. Appl. Crystallogr.* **1999**, *32*, 837−838.

DOI: 10.1021/acs.inorgchem.7b00206
Inorg. Chem. 2017, 56, 5089−5095